Characterization of ULF pulsations by THEMIS

T. E. Sarris,[1,2] W. Liu,[1] K. Kabin,[3] X. Li,[1] S. R. Elkington,[1] R. Ergun,[1] R. Rankin,[3] V. Angelopoulos,[4] J. Bonnell,[5] K. H. Glassmeier,[6] and U. Auster[6]

Received 19 November 2008; accepted 15 January 2009; published 24 February 2009.

[1] The THEMIS five-probe constellation was launched in 17 February 2007 to study substorms; however its instrumentation and the alignment at distances $<1R_E$ among some of the THEMIS probes, particularly in the first period of its mission, provides unique opportunities to study ULF pulsations in the magnetosphere. In the case study presented, electric and magnetic field fluctuations are identified as field line resonances and their modes of oscillation are discussed. Phase-difference calculations between probes allow estimates of the mode number of the fluctuations. These observations give an excellent source for the verification of model estimates of frequency and polarization of the various modes of field line resonances.
Citation: Sarris, T. E., et al. (2009), Characterization of ULF pulsations by THEMIS, *Geophys. Res. Lett.*, *36*, L04104, doi:10.1029/2008GL036732.

1. Introduction

[2] Magnetospheric electric and magnetic perturbations in the Pc4 and Pc5 range of ULF frequencies, 2 to 25 mHz [*Jacobs et al.*, 1964] can have significant influence on energetic particles in the magnetosphere, which have drift frequencies comparable to this range. However, not all classes of ULF waves are equally important for electron acceleration: simulations by, e.g., *Elkington et al.* [2003] and *Ukhorskiy et al.* [2005] suggest that electrons can be adiabatically accelerated through a drift-resonance interaction with either azimuthal (toroidal) mode or radial (poloidal) mode ULF waves with a different efficiency, depending on the global characteristics of ULF waves. In the non-axisymmetric outer regions of the magnetosphere, both toroidal and poloidal-mode waves may cause transport in association with the respective radial and azimuthal drift motions of the particle. In the axisymmetric inner regions of the magnetosphere, the azimuthal drift is dominant; here, only the poloidal mode will significantly change the particle dynamics. Thus it is particularly important that the spatiotemporal characteristics of the toroidal and poloidal modes in the inner magnetosphere are well understood and characterized.

[3] The frequency spectrum of the guided ULF waves in the terrestrial magnetosphere has been studied extensively using ground-based and satellite measurements as well as models; however the polarization and mode structure of ULF waves, in contrast to their frequencies, is much harder to assess theoretically (see discussion by *Kabin et al.* [2007]). A recently developed cold-plasma model of *Rankin et al.* [2006] and *Kabin et al.* [2007] is able to compute the wave polarization self-consistently for free oscillations of individual field lines, for arbitrary magnetic field topology. Wave frequencies computed using this model have been found to be in agreement with ground-based measurements, but the predicted polarizations have not been compared yet with any satellite measured data. Here we show that the THEMIS mission [*Angelopoulos*, 2008] provides an ideal tool for characterizing ULF pulsations and for testing existing models of Field Line Resonances (FLRs): the five micro-satellites of the THEMIS mission (hereafter termed "probes" A through E) are arranged to study the timing and evolution of substorms but in this paper are utilized to investigate important properties of magnetospheric ULF pulsations through simultaneous measurements of the electric and magnetic field signatures at the various probes. Whereas there have been several studies based on satellite magnetometer data which show a broad region where resonances persist for long periods of time [e.g., *Anderson et al.*, 1990; *Lessard et al.*, 1999], and several ground based studies, which usually show only a narrow region supporting the resonance (see discussion by *Hughes* [1994]), we present here a unique observation with both magnetometer and electric field instruments of an extended region of FLRs from the plasmasphere to the magnetopause.

2. Observations

[4] The first phase of the THEMIS mission, from 15 February to 15 September 2007, is termed the "coast" phase; during this time all five probes are lined up in the same elliptical orbit around the Earth with an apogee of 15.4 R_E. At each orbit the probes cross the plasmasphere, magnetosphere and magnetosheath. In this study we use THEMIS electric and magnetic field measurements from the Electric Field Instrument, EFI [*Bonnell et al.*, 2008] and the Flux Gate Magnetometer, FGM [*Auster et al.*, 2008] during an outbound pass of the five probes on 4 September 2007 from 04:00 to 10:00 UT, as shown in Figure 1. Measurements from EFI onboard probe D are shown in Figures 2a and 2c, where the radial and azimuthal electric field components E_r and E_φ are plotted with a 3 s resolution (spin period). EFI performs measurements by use of two pairs of long wire booms ($\sim$40 and 50 m respectively)

[1]Laboratory for Atmospheric and Space Physics, University of Colorado, Boulder, Colorado, USA.
[2]Space Research Laboratory, Demokritus University of Thrace, Xanthi, Greece.
[3]Department of Physics, University of Alberta, Edmonton, Alberta, Canada.
[4]Institute of Geophysics and Planetary Physics, University of California, Los Angeles, California, USA.
[5]Space Sciences Laboratory, University of California, Berkeley, California, USA.
[6]IGEP, Technical University of Braunschweig, Braunschweig, Germany.

0094-8276/09/2008GL036732

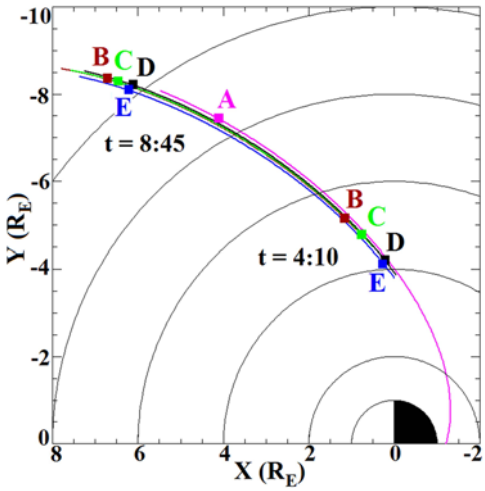

Figure 1. Orbits of the 5 THEMIS probes, A through E, from 04:00 to 10:00 on 4 September 2007. The locations of the probes on 04:10 and 08:45 UT are also shown.

extended in the spacecraft spin plane (∼XY plane in GSE). Figures 2b and 2d below each component give the Dynamic Power Spectra (DPS) for frequencies up to 50 mHz. In both components near-monochromatic Pc5 fluctuations appear at about 04:10 UT and can be observed throughout the orbit, initially at ∼25 mHz and gradually dropping to ∼4 mHz. Consistent signatures were observed by the identical EFI on probes C and E; probes A and B did not have their booms deployed at the time. At 08:42 an instantaneous crossing of the magnetopause at ∼10 R_E is identified by intense fluctuations, by a sharp drop in $B_{//}$ from ∼40 nT to 8 nT and by an increase in low-energy (5 eV to 30 keV) ions as measured by the Electrostatic Analyser (ESA) experiment (measurements not shown). Subsequent magnetopause crossings indicate a ''flapping'' of the magnetopause. Model calculations of predicted FLR frequencies in this region as determined by the Alfvén speed distribution along the field line are plotted on top of the DPS as black and white lines; these indicate that the observed Pc5 pulsations are FLRs, characterised by a gradual drop in frequency as THEMIS-D moves outwards to regions of lower density. A comparison between the electric and magnetic field shows that there is a 90° phase difference (measurements not shown), which is also a characteristic of the presence of a standing wave FLR.

[5] In Figures 2e and 2f measurements of the azimuthal magnetic field B_φ are plotted: fluctuations at frequencies similar to those in the EFI data can be observed, together with their harmonics. No magnetic field pulsations were observed in the field-aligned or radial directions. Components of the magnetic field vector were projected in a Mean Field-Aligned (MFA) coordinate system in order to separate the ULF field variations perpendicular to as well as along the magnetic field direction. Waves in the $\hat{\mathbf{e}}_{//}$, $\hat{\mathbf{e}}_r$ and $\hat{\mathbf{e}}_\phi$ directions are referred to as compressional, poloidal and toroidal respectively; thus mostly toroidal fluctuations in the magnetic field are observed during this time.

[6] During the outbound pass of THEMIS on September 4 2007, mapping of the field lines passing through the probe locations shows conjunctions with several of the Scandina-

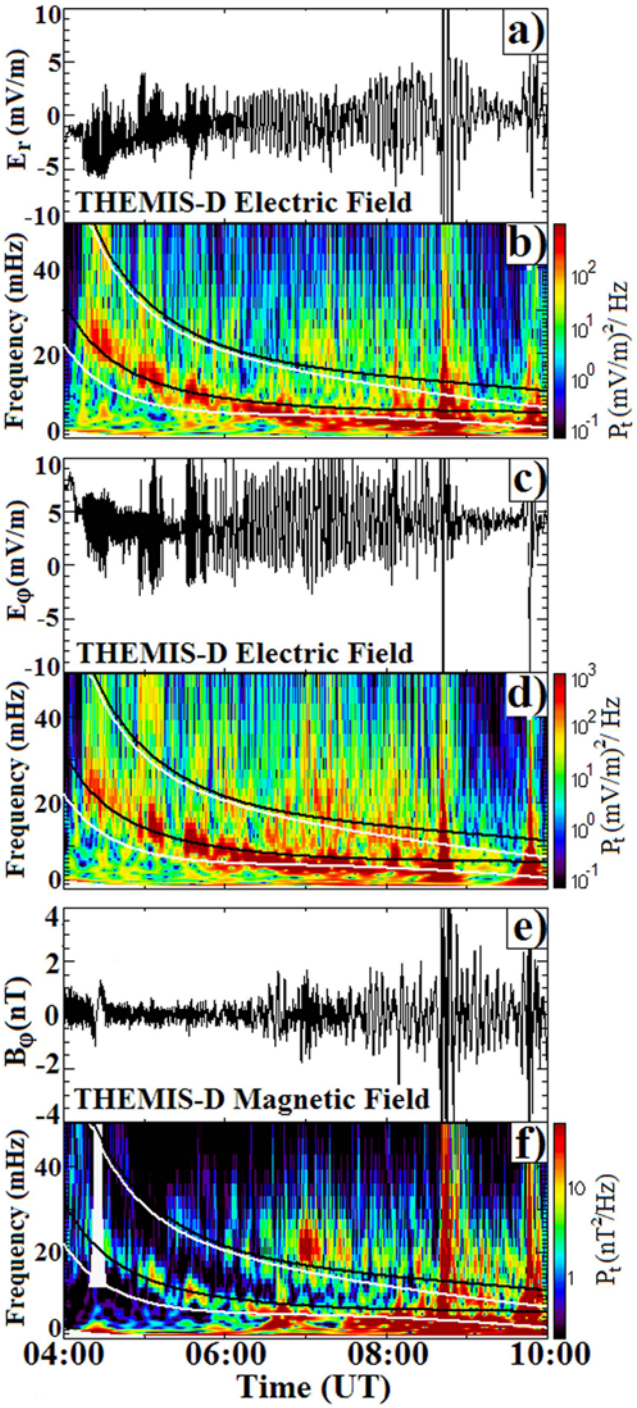

Figure 2. Measurements from THEMIS-D on 4 September 2007: (a) radial component of the electric field, E_r; (b) Dynamic Power Spectra (DPS) of E_r; (c) azimuthal component of the electric field, E_φ; (d) DPS of E_φ; (e) azimuthal component of the magnetic field, B_φ; (f) DPS of B_φ. White lines in Figures 2b, 2d, and 2f show FLR frequencies as calculated using the *Rankin et al.* [2006] model, for the fundamental mode 1 (lower line) and its first harmonic (upper line); black lines show the fundamental mode 2 (lower line) and its first harmonic (upper line).

vian IMAGE ground magnetometers. The DPS of these measurements show broadband Pc5 pulsations mostly in the northward component in the dawn and dusk regions (measurements not shown) which are signatures of Kelvin-Helmholtz shear instability in the magnetosphere flanks. It is thus speculated that the observed FLRs are driven by shear instabilities at the magnetosphere flanks, as described by *Miura* [1987] and *Fujita et al.* [1996].

3. Discussion

3.1. Fundamental and 1st Harmonic Modes of the Observed FLRs

[7] In the following, the *Rankin et al.* [2006] model is used to simulate various modes of fluctuations and predict the frequencies of FLRs, which are then compared to THEMIS-D measurements. Whereas the traditional approach of calculating Alfvénic oscillations of individual magnetic field lines in cold plasma usually involves integrating density along the field line, the *Rankin et al.* [2006] model is based on the covariant-contravariant description of the wave fields, which is necessary because in general there is no orthogonal field aligned coordinate system. Wave polarization is also self-consistently computed in this model. Further discussion of the wave polarization properties are given by *Kabin et al.* [2007]. Using the model of *Rankin et al.* [2006] with realistic T96 magnetic field topology [*Tsyganenko*, 1995], we computed the frequencies and polarizations of the fundamental poloidal and toroidal modes and their first harmonic modes for field lines along the orbit of probe D. In the following, the generalization of the classical poloidal mode will be referred to as ''fundamental mode 1'', whereas the generalization of the classical toroidal mode will be referred to as ''fundamental mode 2''. The computed frequencies of the standing shear Alfvén waves are plotted over the electric and magnetic field DPS in Figures 2b, 2d, and 2f as white lines, representing mode 1 (lower line) and its first harmonic (upper line), and black lines, representing mode 2 (lower line) and its first harmonic (upper line); thus the observed wave more closely resembles a fundamental mode (lower lines). The input parameters in the model were the magnetospheric and solar wind conditions on this day, namely $Dst = -25$ nT, solar wind ram pressure = 1.1 nPa, IMF $B_y = 1$ nT, $B_z = 0$ nT, and the plasma density distribution, which was set to: $\rho = 6 \cdot (5/r)^4$ amu cm^{-3}, where r is the distance from the earth, in R_E. Density here is an adjustable parameter which was chosen to agree with THEMIS ESA density measurements at that time. We note here that, by adjusting the density, one could fit the frequency of some higher harmonic to the data. That, however, would require an unrealistically high plasma density in the magnetosphere, and thus higher harmonics are excluded as a likely possibility. Of the two predicted fundamental modes, the polarizations of the E and B waves point towards the fundamental mode 2, or the toroidal mode (see discussion below). This is also supported by the fact that the magnetic field amplitude of the wave is substantially lower than the corresponding electric field amplitude: such behaviour is expected for fundamental modes near the magnetic equator, where the wave magnetic field has a node and the electric field has an anti-node. Furthermore, confirming the predictions of the model, signatures of a first harmonic are also observed in the THEMIS measurements.

3.2. Polarization of the Observed FLRs

[8] The polarization characteristics of the observed FLRs can be illustrated by hodogram plots showing the variation of the poloidal versus the toroidal components. For example, in Figure 3a a hodogram of the poloidal versus toroidal electric field components is plotted from 6:14 to 6:18 UT. The plotted pulsation has a period of ~160s (6 mHz). At this time E_φ dominates and the polarization is characterized as being mainly azimuthal. In Figure 3b an interesting feature of ULF pulsations is presented: The hodogram plot shows two coupled pulsations with polarizations that are mutually perpendicular. The larger-amplitude pulsation is mostly azimuthal, with a period of 80s (12.5 mHz); coupled to that, a superimposed smaller-amplitude pulsation that is mostly radial, perpendicular to the large-amplitude pulsation, can also be distinguished. The radial pulsation has approximately half the period of the azimuthal pulsation, at ~40s (~25 mHz), indicating a harmonic of the fundamental frequency. Such harmonics or coupled pulsations were observed on several instances throughout the outbound pass of THEMIS-D on this day.

[9] Similar calculations of the direction of polarization were performed for the entire outbound pass of probe D; the calculated magnetic and electric field polarizations along the orbit are plotted in Figures 3c and 3d. Note that electric field polarizations are primarily radial between r = 4 and 6 R_E, then an azimuthal component can also be distinguished from ~6 to ~8 R_E, and turn to mostly radial again at ~9R_E, at about the region where probe D starts observing magnetopause crossings; it is possible that this third region corresponds to the low-latitude boundary layer, the region where transfer of plasma, momentum and energy from the magnetosheath into the magnetosphere occurs.

[10] Polarizations along the THEMIS orbit can also be calculated using the model of Rankin et al.: model magnetic and electric field polarizations for the two fundamental modes 1 and 2 are shown in Figures 3e and 3f and Figures 3g and 3h, marked as m1 and m2 respectively. Model results show that polarization of the various modes changes considerably along the trajectory of probe D. The deviations from the radial and azimuthal directions increase with the distance from the Earth, as the geomagnetic field lines become more disturbed and less dipolar. Out of the predicted modes, m2 (fundamental mode 2) or the generalization of the classical toroidal mode appears to have most similarities to the measured polarizations. Some discrepancies that appear, particularly in the outer parts of the orbit, likely reflect some limitations of the model, which neglects coupling to the compressional mode and the effect of finite ionospheric conductivity (Pedersen and Hall). It is also difficult to assess the accuracy with which the T96 model represents the topology experienced by the THEMIS probes. In light of these uncertainties, the agreement between the model and observations is encouraging.

3.3. Mode Number and Propagation Characteristics of Observed FLRs

[11] The configuration of the THEMIS probes allows the investigation of the azimuthal mode number of the pulsa-

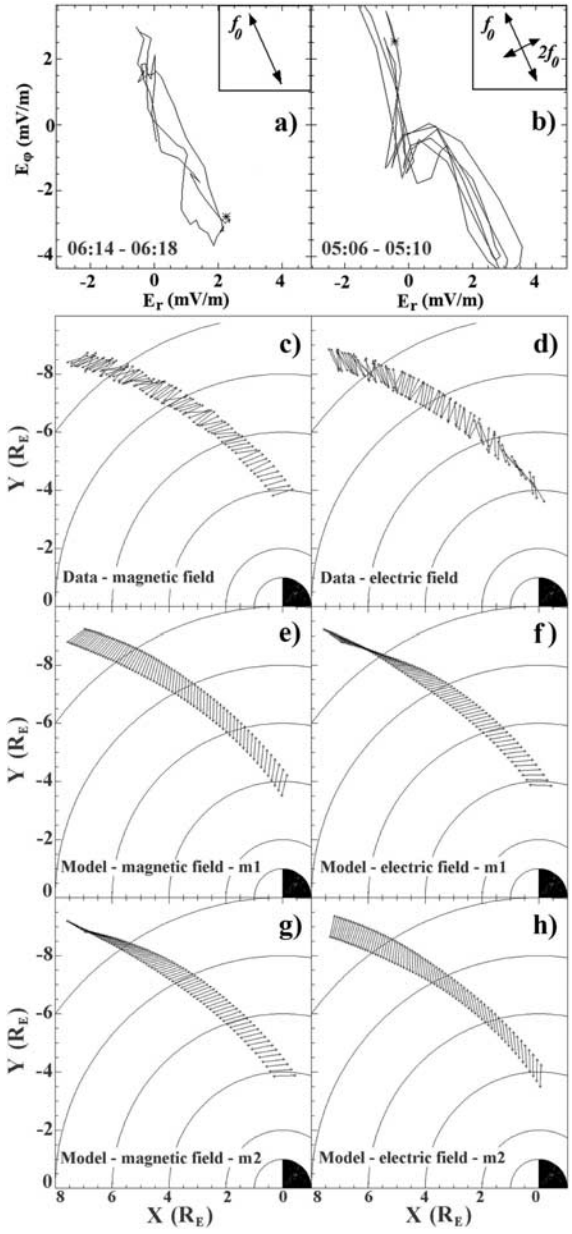

Figure 3. (a) Hodogram of E_φ versus E_r showing a mostly azimuthally polarized pulsation. (b) An azimuthally polarized pulsation is coupled to a radially polarized pulsation at about twice the frequency. (c) Measurements of magnetic field polarization by THEMIS-D. (d) Measurements of electric field polarizations. (e) Model magnetic field polarizations calculated along THEMIS-D orbit using the *Rankin et al.* [2006] model: fundamental mode 1. (f) Model electric field polarizations, fundamental mode 1. (g) Model magnetic field polarizations, fundamental mode 2. (h) Model electric field polarizations, fundamental mode 2.

tions, through monitoring the phase differences between the various probes when they are azimuthally separated. Thus, in Figure 4a using measurements of E_r we calculate the cross-spectral phase differences between probes E & D. In this calculation the Software for Waveform ANalysis (SWAN) designed for the visualization and analysis of scientific and engineering data was utilized [*Lagoutte et al.*, 2000]. The method used is based on classical cross-spectrum estimation, described by, e.g., *Jenkins and Watts* [1969]. A threshold has been used to reveal only the frequencies and time of maximum cross-correlation between the two signals; the threshold has been set at 0.025, meaning that data of cross-spectrogram phase were displayed when power at a frequency bin was above 2.5 percent of the total cross-spectrogram power at that time. The color scale corresponds to the phase differences in degrees. In this figure a consistent phase difference between probes E & D can be distinguished throughout the outbound pass. The measured phase differences, $\Delta\varphi$ between probes E & D are also shown numerically in Figure 4b; the average phase difference for a given time interval is plotted with a star. The line plotted through these values indicates that there is a clear bias towards positive phase differences between probes E & D, indicating that probe E leads consistently the phase of probe D, or that the wave propagates in a westward, or anti-sunward direction in the dawn region. Figure 4c gives the azimuthal separation, $\Delta\lambda$ between probes E & D. In Figure 4d the mode number m is calculated from $m = \Delta\varphi/\Delta\lambda$. The average value for m is $\sim$13, and is indicated by a red dashed line. This is consistent with the range of m values calculated through MHD simulations by *Claudepierre et al.* [2008] due to shear interactions in magnetosphere flanks.

4. Summary and Conclusions

[12] This paper reports the first use of THEMIS to determine the polarization properties of ULF waves in a non-dipolar magnetic topology. The frequencies and polarizations of the second (toroidal) mode predicted by the ULF models of *Rankin et al.* [2006] and *Kabin et al.* [2007] are found to agree well with data. The measured wave frequency

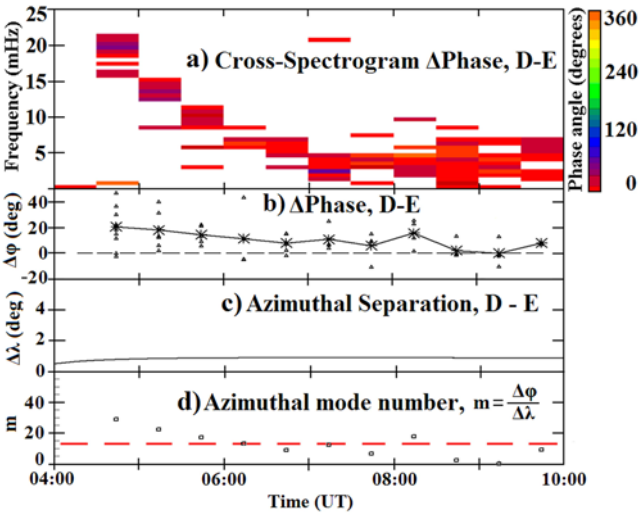

Figure 4. (a) Phase differences between E_r from probes E & D, for frequencies of maximum cross-spectrogram power. (b) Numerical values of the phase differences, $\Delta\varphi$ between probes E & D (stars: average value at each time bin). (c) Azimuthal separation, $\Delta\lambda$ between E & D. (d) Mode number of the resonances, $m = \Delta\varphi/\Delta\lambda$ (dashed line: average m value, $|m| \sim 13$).

varies across *L*-shells in a manner consistent with the model prediction and the phase difference between the electric and magnetic field are found to be 90°, suggesting that the observed ULF waves are free oscillations of the field lines. The demonstrated ability of the THEMIS probes to measure ULF wave polarization and frequencies and to validate and constrain ULF wave models is important for a variety of reasons, including improved understanding of the dynamics of radiation belt particles, as the orientation of the ULF wave polarization with respect to the geomagnetic field determines the efficiency of electron energization by ULF wave processes.

[13] **Acknowledgments.** We thank NASA NAS5-02099 and NSF ATM-0549093 contracts for support of this work. R. Rankin and K. Kabin receive financial support from the Canadian Space Agency and NSERC.

References

Anderson, B. J., M. J. Engebretson, S. P. Rounds, L. J. Zanetti, and T. A. Potemra (1990), A statistical study of Pc 3-5 pulsations observed by the AMPTE/CCE magnetic fields experiment: 1. Occurrence distributions, *J. Geophys. Res.*, *95*, 10,495–10,523.

Angelopoulos, V. (2008), The THEMIS mission, *Space Sci. Rev.*, *141*, 5–34, doi:10.1007/s11214-008-9336-1.

Auster, U., et al. (2008), The THEMIS fluxgate magnetometer, *Space Sci. Rev.*, *141*, 235–264, doi:10.1007/s11214-008-9365-9.

Bonnell, J. W., et al. (2008), The Electric Field Instrument (EFI) for THEMIS, *Space Sci. Rev.*, *141*, 303–341, doi:10.1007/s11214-008-9469-2.

Claudepierre, S. G., S. R. Elkington, and M. Wiltberger (2008), Solar wind driving of magnetospheric ULF waves: Pulsations driven by velocity shear at the magnetopause, *J. Geophys. Res.*, *113*, A05218, doi:10.1029/2007JA012890.

Elkington, S. R., M. K. Hudson, and A. A. Chan (2003), Resonant acceleration and diffusion of outer zone electrons in an asymmetric geomagnetic field, *J. Geophys. Res.*, *108*(A3), 1116, doi:10.1029/2001JA009202.

Fujita, S., K.-H. Glassmeier, and K. Kamide (1996), MHD waves generated by the Kelvin-Helmholtz instability in a nonuniform magnetosphere, *J. Geophys. Res.*, *101*, 27,317–27,325.

Hughes, W. J. (1994), Magnetospheric ULF waves: A tutorial with a historical perspective, in *Solar Wind Source of Magnetosphere Ultra-Low-Frequency Waves*, *Geophys. Monogr. Ser.*, vol. 81, edited by M. J. Engebretson, K. Takahashi, and M. Scholer, pp. 1–11, AGU, Washington, D. C.

Jacobs, J. A., Y. Kato, S. Matsushita, and V. A. Troitskaya (1964), Classification of geomagnetic micropulsations, *J. Geophys. Res.*, *69*, 180–181.

Jenkins, G. M., and D. G. Watts (1969), *Spectral Analysis and Applications*, Holden-Day, San Francisco, Calif.

Kabin, K., R. Rankin, I. R. Mann, A. W. Degeling, and R. Marchand (2007), Polarization properties of standing shear Alfvén waves in non-axisymmetric background magnetic fields, *Ann. Geophys.*, *25*, 815–822.

Lagoutte, D., J. Brochot, and P. Latremoliere (2000), SWAN, software for wave analysis, version 2.4, technical report, Lab. of Phys. Chim. Environ., Orléans, France.

Lessard, M. R., M. K. Hudson, and H. Lühr (1999), A statistical study of Pc3–Pc5 magnetic pulsations observed by the AMPTE/Ion Release Module satellite, *J. Geophys. Res.*, *104*, 4523–4538.

Miura, A. (1987), Simulation of Kelvin-Helmholtz instability at the magnetospheric boundary, *J. Geophys. Res.*, *92*, 3195–3206.

Rankin, R., K. Kabin, and R. Marchand (2006), Alfvénic field line resonances in arbitrary magnetic field topology, *Adv. Space Res.*, *38*, 1720–1729.

Tsyganenko, N. A. (1995), Modeling the Earth's magnetospheric magnetic field confined within a realistic magnetopause, *J. Geophys. Res.*, *100*, 5599–5612.

Ukhorskiy, A. Y., K. Takahashi, B. J. Anderson, and H. Korth (2005), Impact of toroidal ULF waves on the outer radiation belt electrons, *J. Geophys. Res.*, *110*, A10202, doi:10.1029/2005JA011017.

V. Angelopoulos, Institute of Geophysics and Planetary Physics, University of California, 3845 Slichter Hall, 603 Charles E. Young Drive East, Los Angeles, CA 90095, USA.

U. Auster and K. H. Glassmeier, IGEP, Technical University of Braunschweig, Mendelssohnstr. 3, D-38106 Braunschweig, Germany.

J. Bonnell, Space Sciences Laboratory, University of California, 7 Gauss Way, Berkeley, CA 94720, USA.

S. R. Elkington, R. Ergun, X. Li, and W. Liu, Laboratory for Atmospheric and Space Physics, University of Colorado, 1234 Innovation Drive, Boulder, CO 80303, USA.

K. Kabin and R. Rankin, Department of Physics, University of Alberta, 11322 89 Avenue, Edmonton, AB T6G 2J1, Canada.

T. E. Sarris, Space Research Laboratory, Demokritus University of Thrace, Vassilisis Sofias 1, GR-67100 Xanthi, Greece. (tsarris@ee.duth.gr)